

# Study of the Effects of Mechanical Alloying on 2024 Al-SiC<sub>p</sub> composite

Satish Tailor<sup>1</sup>, V K Sharma<sup>1</sup>, P.R. Soni<sup>1</sup>, R.M. Mohanty<sup>2</sup>

<sup>1</sup>Department of Metallurgical and Materials Engineering, Malaviya National Institute of Technology

<sup>2</sup>Council of Scientific and Industrial Research (CSIR), New Delhi, INDIA

2024 Aluminum alloy with 15Wt% SiC particulate composite was produced by P/M processing. Mechanical alloying (MA) technique was used to mill the blended powder under purified nitrogen. The results of MA processing have been investigated with SEM, EDAX and XRD. The results show that the matrix particle size and crystallite size reduced after MA and homogeneous distribution of SiC<sub>p</sub> reinforcement in the matrix could be obtained. The MA processing also results in cold worked structure, contamination due to oxygen, iron and carbon in the matrix.

Keywords: MECHANICAL ALLOYING; PM PROCESSING; ALUMINUM ALLOY-SiC<sub>p</sub> COMPOSITE; SiC HOMOGENEOUS DISTRIBUTION.

## Introduction

Aluminum based metal matrix composites are used in aerospace, defence and selected automotive applications such as high performance racing applications [1]. The most commonly used materials as reinforcement are SiC, Al<sub>2</sub>O<sub>3</sub> or B<sub>4</sub>C into the aluminum matrix. These materials are used to improve elastic modulus, enhanced heat and wear resistance [2]. The attritor, which is effectively a high energy ball mill containing internally agitated media, is widely used to disperse reinforcement in the P/M matrix. The most important concept in the attritor is that the power input is used directly for agitating the media to achieve grinding and is not used for rotating or vibrating heavy tank in addition to the media [3]. While applying the technique for dispersoid distribution, it is known as mechanical alloying (MA). Though, it is not really 'alloying' due to insolubility of the dispersoids in the matrix [4]. Mechanical alloying, as originally developed by Benjamin, was used to produce a combined oxide dispersion strengthening with gamma prime precipitation hardening in a nickel-based superalloy [5].

The purpose of the present studies is to investigate the influence of MA processing on the particle size, crystallite size and microstructural changes in powder particles and distribution of SiC<sub>p</sub> reinforcement and their corresponding properties.

## Methodology

2024 Al alloy powder supplied by the M/S EKCA Granulate Veldem GmbH, Germany, with a particle size of <71µm, and the silicon carbide powder with an average particle size of 10-15 µm were used in these investigations. The chemical composition of the 2024Al powder is shown in Table 1.

As-received 2024 Al powder was mechanical alloyed with 15wt% SiC particles in a high energy attrition mill for 8 h with a rotation speed of 350 rpm. The milling media used was stainless steel balls of 12.2mm dia. The weight ratio of milling media to powder was 10:1. Acrawax C was used as a process control agent (PCA). Milling was carried out in purified nitrogen to prevent oxidation during milling. These mechanical alloying parameters have been summarized in Table 2. The MA powder was then degassed at temperature of 200<sup>0</sup> C, in vacuum oven at 10<sup>-2</sup> torr.

**Table 1.** The Chemical Composition of 2024Al Powder (Wt%)

Component	Wt. %
Al	Balance
Cr	Max 0.1
Cu	3.8 - 4.9
Fe	Max 0.5

Mg	1.2 - 1.8
Mn	0.3 - 0.9
Si	Max 0.5
Ti	Max 0.15
Zn	Max 0.25
Other, each	Max 0.05
Other, total	Max 0.15

**Table 2.** Mechanical Milling Parameters

Parameter	Details
RPM	350
Grinding media	hardened steel balls (dia.-12.2 mm)
Ball to charge ratio	10:1
Atmosphere	purified nitrogen
Process Control Agent (PCA)	2Wt% Acrawax C (2gm)
Milling Time	8hr

Particle size analyses were carried out by CILAS analyzer. The morphologies and distribution of the SiC particles and compositional analysis were carried out using TESCAN scanning electron microscope (SEM) with energy-dispersive X-ray analyzer (EDAX). For phases analysis Philips X-Part X-ray diffraction unit with  $\text{Cu}_{K\alpha}$  radiation ( $k_{\alpha}=0.1542\text{nm}$ ) was used.

## Results and Discussion

### *Morphologies of particles and their size evolution*

**Figures 1 (a)** and **(b)** show the particle size distribution of milled 2024 and 2024+15Wt%SiC. The particle sizes  $D_{0.5}$  in mechanically alloyed 2024 and 2024+15Wt%, are  $32.65\mu\text{m}$  and  $13.71\mu\text{m}$  respectively. This reduction in particle size from as received powder particle size  $<71\mu\text{m}$  due to mechanical alloying.

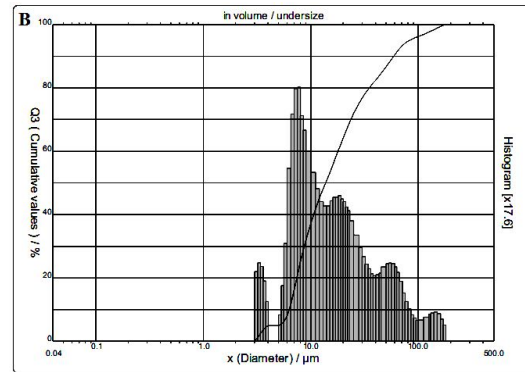
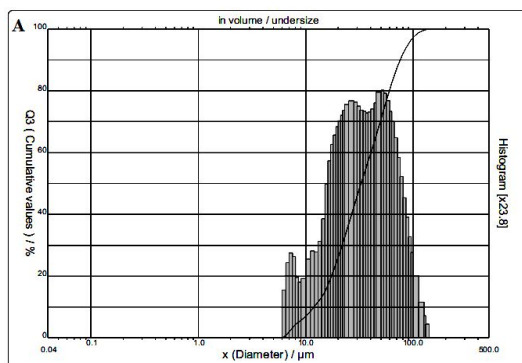


**Figure 1.** The particle size distribution of (a) Milled 2024 and (b) Mechanical alloyed 2024/SiC<sub>p</sub>

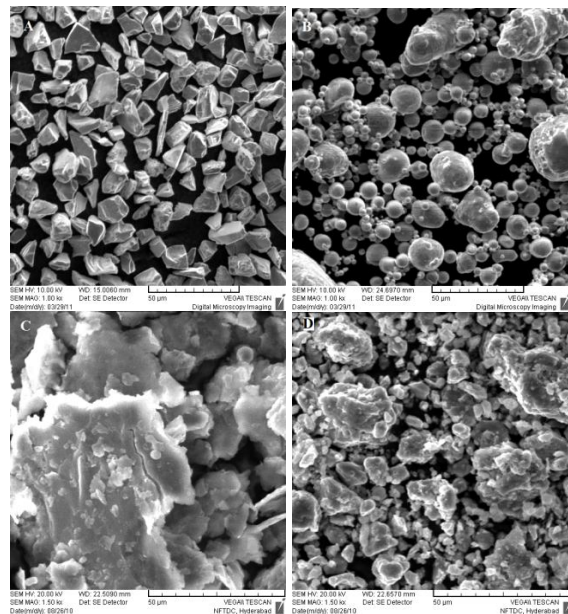


**Figure 2.** The powder morphologies: (a) SiC powder; (b) SEM of as received 2024Al (c) SEM of milled 2024Al (d) SEM of MA 2024Al/SiC<sub>p</sub> showing embedded SiC<sub>p</sub>

Scanning electron micrographs of as received SiC particles, 2024Al and milled and MA 2024Al are shown in Fig.2 It can be seen that the SiC particles have irregular shape and sharp angles and the initial spherical shape of the 2024Al powder has become irregular shaped after MA, with the small particles also flattened and attached to the large particle (**Figure 2c**) and also the SiC<sub>p</sub> particles get embedded in the matrix powder (**Figure 2d**). Refinement of particles is seen in 2024Al when milled with SiC<sub>p</sub>. At the time of mechanical alloying the small particles collided with the large particle, and then were cold-welded. At same time, the assembled particle was broken when the collision force was large enough to exceed the compressive strength of the particle [6].

### *X-ray diffraction pattern*

**Figure 3** and **Figure 4** shows the XRD patterns of as received 2024Al, milled 2024Al and MA 2024Al+15Wt%SiC. The XRD patterns show a decrease in peak intensity and an increase in peak width after MA, indicating a change in crystallite size. Fig. 4 shows shifting of the main peak to higher  $2\theta$  angle indicates the existence of strain in the MA matrix powder. Thus the line broadening of the main peak is due to both stresses and grain size reduction caused by MA [7]. The crystallite size calculated by the following Scherrer equation which gives the peak broadening due to crystallite size

$$B(2\theta) = \frac{0.94\lambda}{L \cos\theta} \dots\dots\dots \text{Eqn. 1.}$$

Where B is peak width and L crystallite size. The crystallite size in as received 2024Al, milled 2024Al and MA 2024Al/SiC<sub>p</sub> are 102 nm, 73 nm and 45 nm respectively.

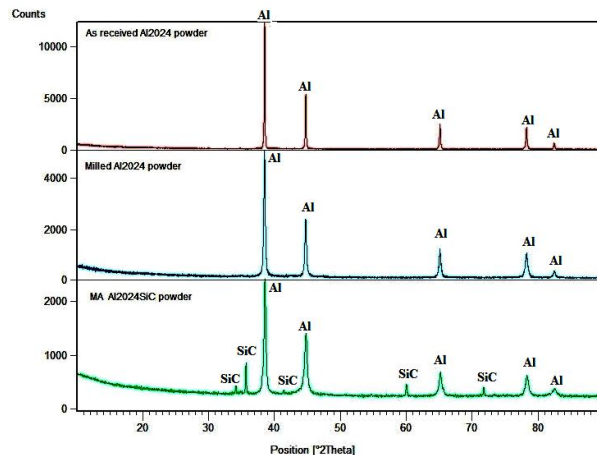


**Figure 3.** XRD patterns of as received 2024Al, Milled 2024Al, MA 2024AlSiC

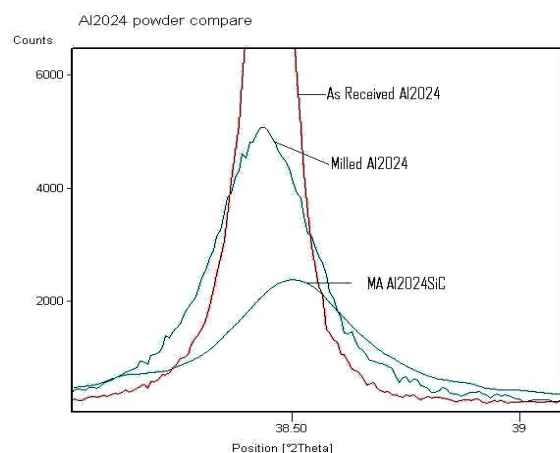


**Figure 4.** Effect of mechanical alloying

A powder weight change experiment was performed to investigate the gas and moisture absorbed during MA (**Figure 5**).

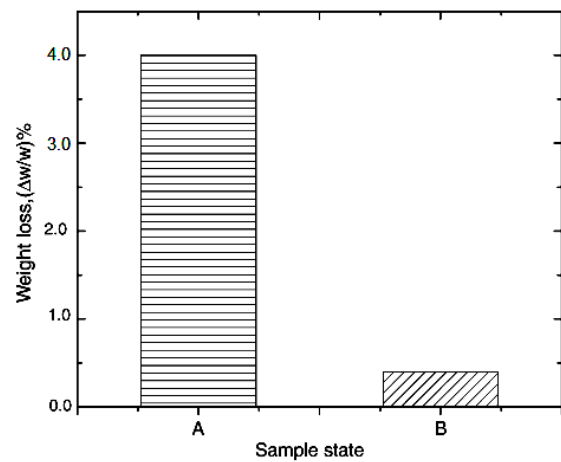


**Figure 5.** Weight changes of MA 2024Al/SiC<sub>p</sub> powder; (A) Weight loss after degassing treatment at 200<sup>0</sup> C (B) Weight gain by degassed powder after exposure in air for 24 h

A powder weight change experiment was performed to investigate the gas and moisture absorbed during MA. The weight loss of MA 2024Al/SiC<sub>p</sub> powder was 4wt% after heating in vacuum at 200<sup>0</sup> C for 1 h; while the weight gained by the degassed powder was only about 0.4wt% after exposure to the air for 24 h (**Figure 5**). Thus powder adsorbed about 4wt% gases, during the MA processing, which may include O<sub>2</sub>, moisture and N<sub>2</sub>, oxygen will most likely be combined as Al<sub>2</sub>O<sub>3</sub> and is not removable by degassing treatment.

EDS analysis [**Figure 6**] indicate some contamination of the MA powder with oxygen, iron from the milling media, and carbon resulting due to decomposition of the Acrawax C used as a PCA. These contaminants may affect the compressibility and sintering characteristics of the powder [8].

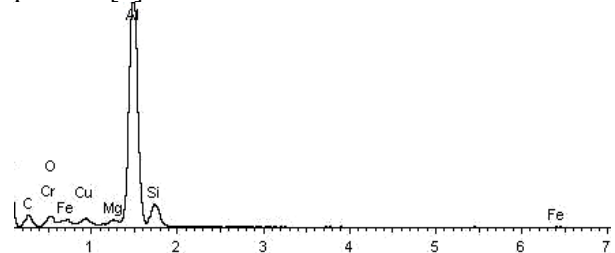


**Figure 6.** EDS analysis of the MA 2024Al/SiC powder

According to the above experiments, the MA processing could have advantageous to obtain a

composite with uniform reinforcement distribution, but the disadvantages are obvious [9].

## Conclusions

SiC particles dispersed 2024Al alloy matrix was synthesized using MA technique. These investigations show that:

1. A relatively homogeneous distribution of SiCp reinforcement in the finer 2024Al matrix could be obtained by mechanical alloying technique.

2. MA processing also results in cold worked structure, contamination due to oxygen, iron and carbon in the matrix.

3. Crystallite size in matrix of nanometre.

## References

1. Hurley S, MMCs Find Broad Range of Niche Markets, 1995, Met. Bull. Mon., pp. 54–56.
2. Otsuki M S, Kakehashi S, Kohno T, Powder Forging of Rapidly Solidified Aluminum Alloy Powders and Mechanical Properties of Their Forged Parts, in: Advances in Powder Metallurgy, vol. 2, Metal Powder Industries Federation, Princeton, NJ, 1990, pp. 345–349.
3. Lu L, Lai M O, Ng C W, Enhanced Mechanical

Properties of An Al Based Metal Matrix Composite Prepared Using Mechanical Alloying, Mater. Sci. Eng. 1998, A 252 (2), pp. 203–211.

4. Sankar R, Singh P, Synthesis of 7075 Al/SiC Particulate Composite Powders by Mechanical Alloying, Mater. Lett., 1998, 36, pp. 201–205.

5. Soni P R, Mechanical Alloying- Fundamentals & Applications, Press: Cambridge International Science Publishing, 2001, 6-23 p.

6. Benjamin J S , Volin T E, The Mechanism of Mechanical Alloying, Metall. Trans. 5, 1974, pp.1929–1934.

7. Gilman P S, Nix W D, The Structure and Properties of Aluminium Alloys Produced by Mechanical Alloying: Powder Processing and Resultant Powder Structures, Metall. Trans. 1981, A 12, pp. 813–823.

8. Naiqin Zhao , Philip Nash, Xianjin Yang, The Effect of Mechanical Alloying on SiC Distribution and The Properties of 6061 Aluminum Composite, Journal of Materials Processing Technology, 2005, 170, pp. 591.

9. Oleg Neikov, Stanislav Naboychenko, Irina Mourachova , Victor Gopienko , Irina Frishberg, Dina Lotsko, Handbook of Non-Ferrous Metal Powders, Technologies and Applications; Press: Elsevier, 2009, 267-283 p.

Received September 21, 2011